EVALUATION OF THE EFFECTIVENESS OF NO REMOVAL USING THE PHOTOCATALYTIC ACTIVATED MATERIAL S-TiO$_2$/DIATOMITE

Le Thi Pho[(1)]

(1) Thu Dau Mot University
Corresponding author: pholt@tdmu.edu.vn

DOI: 10.37550/tdmu.EJS/2024.01.526

Article Info

Volume: 6
Issue: 01
March 2024
Received: Feb. 9th, 2024
Accepted: Mar. 11th, 2024
Page No: 145-150

Abstract

S-TiO2 typically exhibits high photocatalytic activity, but its powdered form makes it difficult to apply practically in environmental pollution treatment. Diatomite from different locations varies in purity and integrity of the diatomaceous earth, making it a suitable catalyst support for synthesizing mixed-phase S-TiO2 catalysts using the sol-gel technique. The synthesized photocatalyst exhibits photocatalytic activity similar to that of S-TiO2. The NO removal efficiency under the same conditions with different catalyst supports only decreases by approximately 3% within 30 minutes at a reaction rate of 0.0950 min-1, with an optimal mass ratio of 70:30 for S-TiO2 and diatomite. This composite material holds promise for addressing the application of photocatalytic materials in practical environmental treatment, including NO removal and the treatment of other environmental pollutants, as diatomite is a naturally available and environmentally friendly material.

Keywords: diatomite, NO removal, photocatalysis, S-doped TiO2 nanotube, sol-gel technique

1. Introduction

International issues include environmental pollution, global warming, and the lack of clean and eco-friendly energy sources. Scientists and technologists worldwide are researching various methods to address ecological concerns. One of the currently highly prioritized methods is photocatalysis, utilizing the exceptional properties of semiconductor materials to completely oxidize organic compounds using air oxygen as the catalyst under the influence of solar light. Therefore, a crucial requirement is to search for photocatalysts that work effectively in the visible light region (Karthikeyan et al., 2020).

One of the semiconductor photocatalysts utilized for catalyzing the degradation of water and organic pollutants in the air is titanium dioxide (TiO_2) (Bian et al., 2024; Gopinath et al., 2020). It is widely employed due to its stable physical and chemical properties, high catalytic activity, and ease of synthesis. Numerous studies have shown that modifying TiO_2 with certain metallic and non-metallic elements can reduce the bandgap energy, thereby expanding the range of visible light photocatalysis. The key for subsequent applications lies in the material's electronic structure, which includes a wide bandgap of 3.2 eV, appropriate edge positions for various oxidation-reduction reactions, a relatively long lifetime of excited electrons, and special photostability. While the wide bandgap is crucial for many applications, it also limits the use for solar irradiation-controlled applications (only 7% of solar energy is supplied within the < 400 nm spectral range, meaning the super-wideband energy range of TiO_2) (Samsudin & Abd Hamid, 2017; Wang et al., 2024). Therefore, research is focused on modifying the electronic properties of TiO_2 through techniques such as bandgap engineering (narrowing the optical bandgap) and incorporating large quantities of impurities with elements such as S, N, or metals to create visible light-responsive photocatalytic reactions (Akhter et al., 2022; Basavarajappa et al., 2020; Orizu et al., 2023).

However, TiO_2 and its impurity phases are typically powders, which pose challenges in practical applications. Therefore, selecting a readily available material from nature to assist in forming composite structures for practical applications while having minimal impact on the photocatalytic activity of TiO_2 and its impurity phases is necessary (Ao et al., 2019; Jin et al., 2022).

Diatomite is widely used in construction, the petroleum industry, the light industry, the chemical industry, and other fields, thanks to its unique physical and chemical properties. The distinctive characteristics of diatomite, such as its porous and multi-layered structure, make premium diatomite resources increasingly scarce. In Vietnam, diatomite is a sedimentary rock mainly found in Phu Yen, Lam Dong, and An Giang provinces. Some main minerals in diatomite include diatom shells, opal, clay, and sea sponge spicules (Nguyen & Dang, 2020; Van Viet et al., 2020). Its crystal structure in Phu Yen is in tubes or long cylinders, making it highly porous (Son et al., 2017). Currently, diatomite is widely applied as a filter aid material and used in shrimp farming water treatment, as a raw material in the production of insulation materials, as an additive in the production of cement and lightweight concrete, and more. However, diatomite's full potential and environmental applications have not yet been fully exploited, and there are limited studies on diatomite in ecological treatment (Chen & Liu, 2016; Jin et al., 2022).

This study aims to create the initial composite of S-TiO_2/Diatomite to preserve the photocatalytic efficiency while incorporating diatomite as a nano S-TiO_2 carrier material.

2. Materials and methods

2.1. *Materials*

• Diatomite-prepared diatomite material in Phu Yen province

• Research chemicals: NaOH (China, 96%), HCl (China, 36%), pure TiO_2 (China, 98%), Thioure (China, 99%)

2.2. Methods

Preparation of diatomite:

Diatomite is mixed with 5M HCl acid in a ratio of 1:25 and stirred at 1000 rpm at 75°C for 72 hours. Afterward, it is thoroughly rinsed with deionized water multiple times until the pH value reaches 7. Finally, the sample is dried at 80°C for five hours (Alyosef et al., 2014).

Synthesis of S-TiO_2/Diatomite:

The S-TiO_2/Diatomite composite is synthesized through the sol-gel method. Firstly, 0.5g of S-TNTs is weighed and mixed with 20mL ethanol while stirring. This solution is designated as solution A. To prepare solution B, diatomite and ethanol are mixed in different weight ratios (30%, 40%, 50%, 60%), 0.5mL of glacial acetic acid, and 1.5mL nitric acid (1 mol/l) while stirring the mixture. Solution B is gradually added to solution A with continuous stirring to obtain the precursor gel. The precursor gel is then dried at 60°C and annealed at 500°C for 2.5 hours to form the S-TiO_2/Diatomite composite.

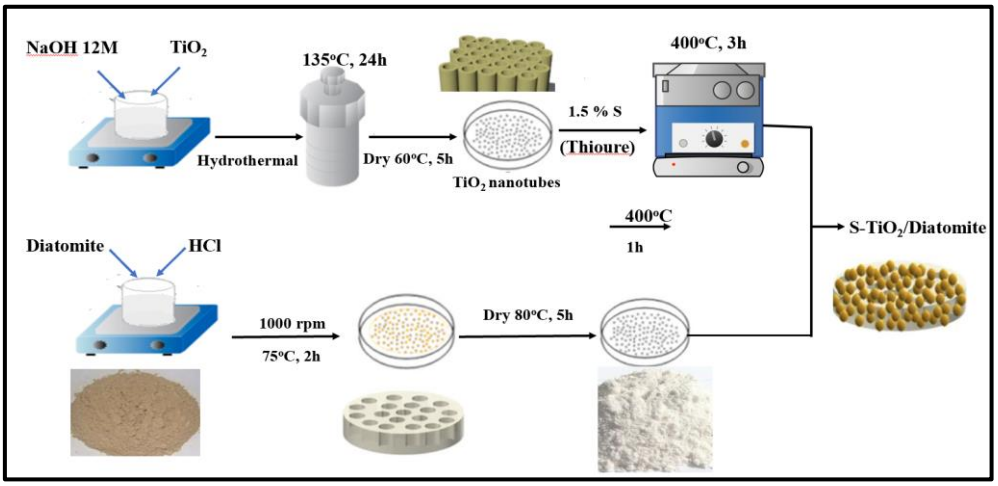

Fig 1. Material synthesis process S-TiO_2/Diatomite material

Evaluate the NO gas treatment efficiency of photocatalytic materials.

To treat NO gas using the S-TiO_2/Diatomite material, we utilize a solar simulator lamp (OSRAM 300 W) as the light source, which emits wavelengths ranging from 400 to 800nm.

0.2g of the S-TiO_2/Diatomite material is weighed and placed in a 10cm diameter Petri dish, which is then placed inside the photocatalytic chamber equipped with a UV/IR filter. The flow rate is controlled at 3L/min, and the humidity is maintained at 70%. The photocatalytic catalysts are irradiated for 1 hour to achieve a NO adsorption/desorption equilibrium state in the dark.

The NO removal efficiency (H%) is calculated using the following formula (Van Pham et al., 2022):

$$H\% = \frac{(C_0 - C_t)}{C_0} \times 100\%$$

C_0 and C_t represent the NO concentration in the inlet and outlet streams.

3. Results and Discussion

The investigation on photocatalytic removal of NO with a concentration of 500 ppb in Figure 2a shows that Diatomite does not exhibit photocatalytic activity. However, when Diatomite is combined with S-TiO_2 material, the efficiency of NO gas treatment increases significantly but is still lower than that of S-TiO_2 material alone. The photocatalytic activity increases sharply in the first 7 minutes due to the large contact area and the absence of reaction by-products that hinder the contact between the material and NO gas. After that, the efficiency increases very little until 30 minutes. The samples combined with S-TiO_2 material in ratios of 30%, 40%, 50%, and 60% Diatomite exhibit treatment efficiencies of 44.4%, 43.3%, 41%, and 36.2%, respectively. Therefore, the S-TiO_2-30D% material has the highest NO treatment efficiency, although it is still lower than the efficiency of the S-TiO_2 material alone (47.3%). After combining with Diatomite, the efficiency decreases in the range of 2.9-11%. Both TiO_2 and S-TiO_2 materials are in powder form, which presents some difficulties in practical applications. Thus, this study proposes using high-temperature-resistant Diatomite as a carrier for photocatalytic materials to facilitate practical applications. When Diatomite is combined with S-TiO_2 nanotubes, these particles are attached to the cavities of Diatomite. If the Diatomite content increases, the surface area of S-TiO_2 nanotubes decreases, leading to a tendency to reduce photocatalytic activity. Therefore, the appropriate ratio for Diatomite as a carrier in the composite mixture of Diatomite and S-TiO_2 is 30:70, which exhibits photocatalytic activity. Currently, other studies are exploring the application of Diatomite with various materials in environmental treatment. Wen Sun et al. researched nano-TiO_2/diatomite to remove natural organic matter, achieving promising results (Sun et al., 2014). Zhiming Sun et al. studied TiO_2/diatomite composites to treat Rhodamine B, achieving high efficiency (Sun et al., 2015). Guangxin Zhang et al. investigated nano-TiO_2/diatomite composites for formaldehyde treatment (Zhang et al., 2016).

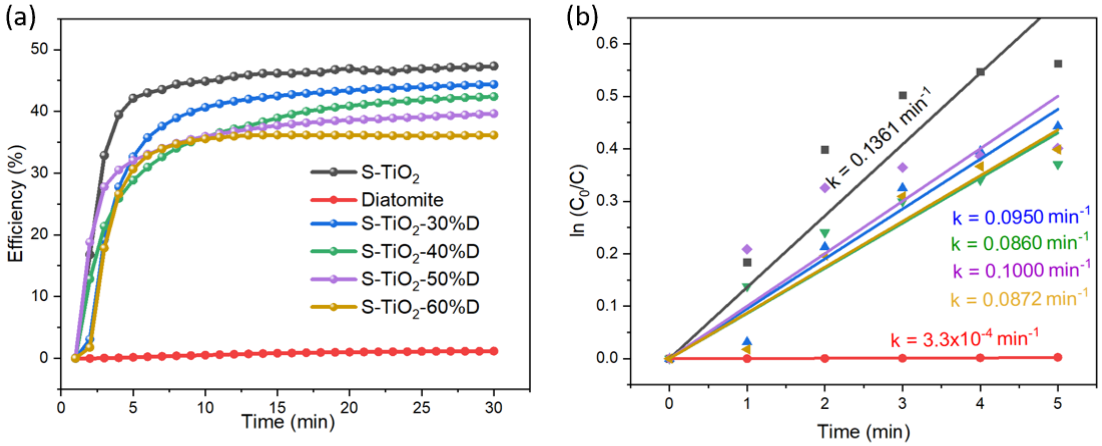

Fig 2. NO gas treatment efficiency depends on time (a) and corresponding. Pseudo-first-order kinetic curves (b)

$S\text{-}TiO_2/Diatomite + hv \rightarrow S\text{-}TiO_2/Diatomite\ (h^+_{VB} + e^-_{CB})$ (1)

$O_2 + e^-_{CB} \rightarrow \cdot O_2^-$ (2)

$H_2O + h^+_{VB} \rightarrow HO^\cdot + H^+$ (3)

$2\cdot O_2^- + H_2O \rightarrow HO_2^\cdot + OH^-$ (4)

$2\ HO_2^\cdot + H_2O + e^-_{CB} \rightarrow H_2O_2 + OH^-$ (5)

$2\cdot O_2^- + H_2O \rightarrow 2H_2O_2 + O_2$ (6)

$H_2O_2 + e^-_{CB} \rightarrow HO^\cdot + OH^-$ (7)

$NO + \cdot O_2^- \rightarrow NO_3^-$ (8)

$NO + HO^\cdot \rightarrow NO_2 + H_2O$ (9)

The mechanism of photocatalytic activity in the decomposition of NO gas under visible light by S-TiO_2/Diatomite is shown in Figure 4 and described by Equations (1-9). When stimulated by appropriate photon energy, S-TiO_2/Diatomite undergoes the process of photoinduced electron (e^-) and hole (h^+) separation, as shown in Equation (1). Some of the generated electrons (e^-) migrate to the surface of the photocatalyst and reduce the absorbed O_2 molecules to form $\bullet O_2^-$ (Equation (2)). Subsequently, the $\bullet O_2^-$ radicals continuously undergo intermediate reactions with H_2O to produce additional •OH radicals (Equations (4 - 6). Additionally, the trapped holes can oxidize OH^- species to •OH radicals (Equations (3), (7)). Finally, these reactive oxygen species ($\bullet O_2^-$ and •OH radicals) strongly decompose NO gas, as shown in Equations (8) and (9).

The Langmuir-Hinshelwood model is used to explain NO degradation rate in a material through photocatalysis. The first stage of this process shows a linear relationship between the natural logarithm of the ratio of the initial concentration of NO to its concentration at a given time and the reaction time, indicating a first-order kinetic mass transfer-controlled process (Messerer, Niessner, & Pöschl, 2006). The apparent reaction rate constants (k) for S-TiO_2 (0.1361 min^{-1}), S-TiO_2-30%D (0.0950 min^{-1}), S-TiO_2-40%D (0.0860 min^{-1}), S-TiO_2-50%D (0.1000 min^{-1}), S-TiO2-60%D (0.0872 min^{-1}) were determined, while Diatomite, which does not exhibit photocatalytic activity, had a rate constant of 3.3x10-4 min^{-1} (Fig 1b). All the S-TiO_2/Diatomite samples showed lower NO photocatalytic degradation rates than when not mixed with Diatomite.

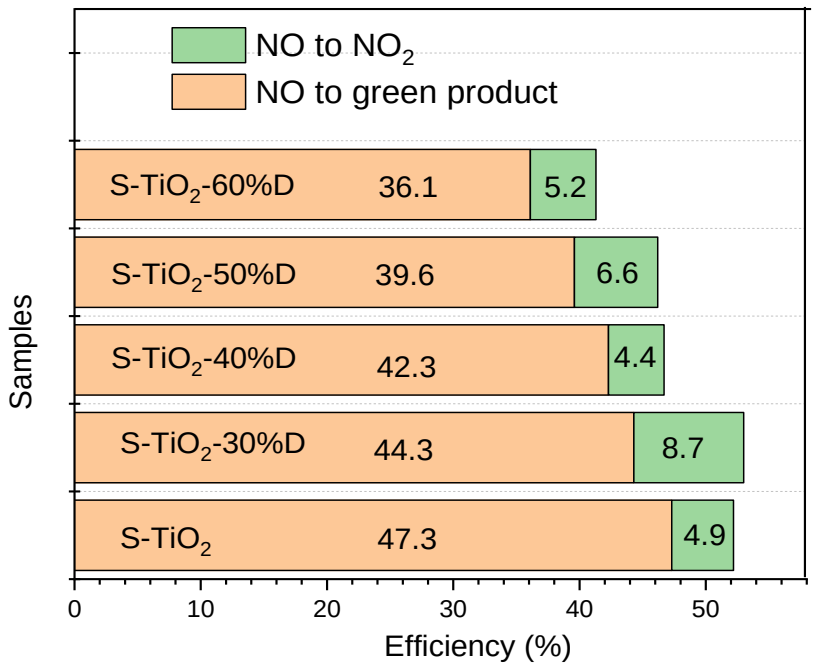

Fig 3. There is NO degradation performance in the green product, NO-to-NO2 conversion of samples.

As shown in Figure 3, the conversion efficiency of NO to NO_2 by S-TiO_2 is relatively low (4.9%), contrary to S-TiO_2-30%D, S-TiO_2-40%D, S-TiO_2-50%D, and S-TiO_2-60%D exhibit conversion efficiencies of 8.7%, 4.4%, 6.6%, and 5.2%, respectively, in the photocatalytic process. This is an unexpected result because NO_2 is more toxic than the initial NO pollutant. The addition of Diatomite to the S-TiO_2 material is believed to contribute to the formation of products, including both NO and NO_2, depending on the amounts of •OH and $•O_2^-$ generated, as described in Equations 4-6.

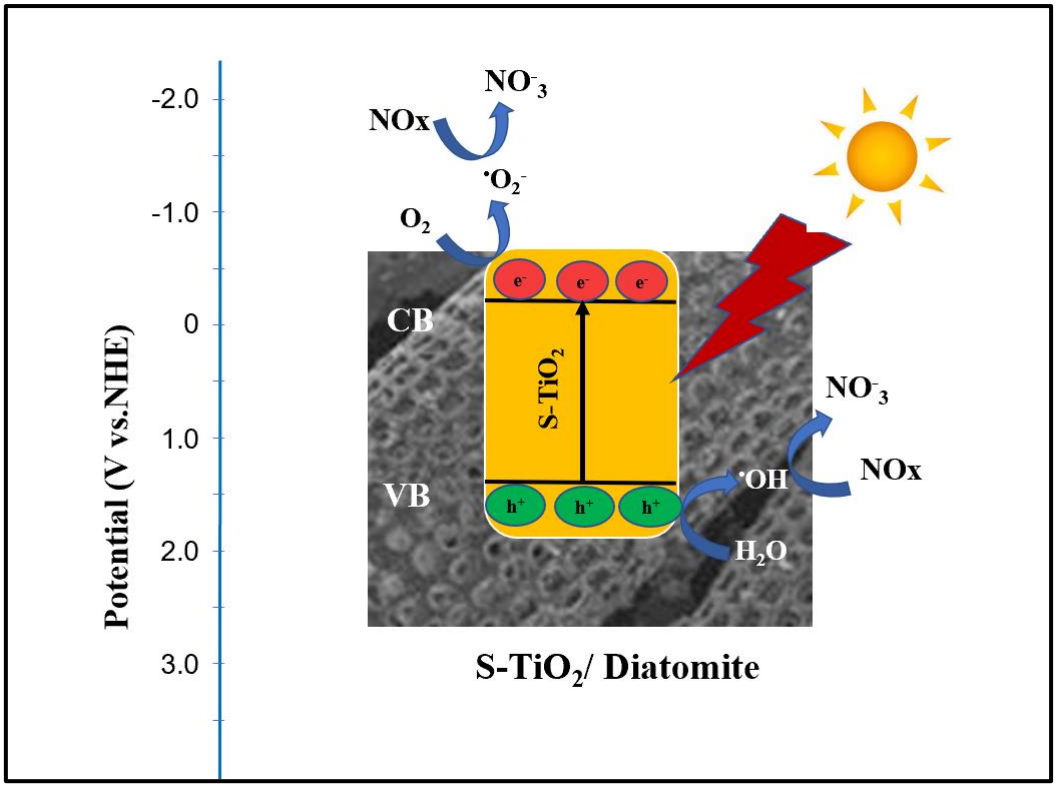

Fig 4. Photocatalytic mechanism illustration of S-TiO_2/Diatomite under visible light illumination

4. Conclusion

In this study, the researcher successfully loaded S-TiO_2 nanoparticles onto diatomite using the sol-gel method. The nano-sized S-TiO_2 particles were dispersed either on the surface or inside the porous structure of diatomite. The ability of the composite catalyst to adsorb depends on the surface area and volume of its pores under ideal circumstances. While the raw diatomite alone had almost negligible photocatalytic activity within 30 minutes of light irradiation, the synthesized composite material exhibited excellent photocatalytic efficiency comparable to S-TiO_2. To apply the S-TiO_2/Diatomite composite in practical applications, further research is necessary on the material's morphology, structure, and recyclability in the future.

References

Akhter, P., Arshad, A., Saleem, A., & Hussain, M. (2022). Recent development in non-metal-doped titanium dioxide photocatalysts for different dyes degradation and the study of their strategic factors: A review. *Catalysts*, *12*(11), 1331.

Alyosef, H. A., Ibrahim, S., Welscher, J., Inayat, A., Eilert, A., Denecke, R., Schwieger, W., Münster, T., Kloess, G., & Einicke, W.-D. (2014). Effect of acid treatment on the chemical composition and the structure of Egyptian diatomite. *International Journal of Mineral Processing*, *132*, 17-25.

Ao, M., Liu, K., Tang, X., Li, Z., Peng, Q., & Huang, J. (2019). BiOCl/TiO_2/diatomite composites with enhanced visible-light photocatalytic activity for the degradation of rhodamine B. *Beilstein Journal of Nanotechnology*, *10*(1), 1412-1422.

Basavarajappa, P. S., Patil, S. B., Ganganagappa, N., Reddy, K. R., Raghu, A. V., & Reddy, C. V. (2020). Recent progress in metal-doped TiO_2, non-metal doped/codoped TiO_2 and TiO_2 nanostructured hybrids for enhanced photocatalysis. *International Journal of Hydrogen Energy*, *45*(13), 7764-7778.

Bian, R., An, S., Wang, X., Xue, Y., Tian, J., Liang, Z., & Song, Z. (2024). Ca^{2+} doped TiO_2 nano-sized polygon plates with oxygen vacancies for photocatalytic hydrogen evolution. *International Journal of Hydrogen Energy*, 51, 787-795.

Chen, Y., & Liu, K. (2016). Preparation and characterization of nitrogen-doped TiO_2/diatomite integrated photocatalytic pellet for the adsorption-degradation of tetracycline hydrochloride using visible light. *Chemical Engineering Journal*, 302, 682-696.

Gopinath, K. P., Madhav, N. V., Krishnan, A., Malolan, R., & Rangarajan, G. (2020). Present applications of titanium dioxide for the photocatalytic removal of pollutants from water: A review. *Journal of environmental management*, 270, 110906.

Jin, H., Chen, H., Qian, X., Jin, W., Du, X., Jin, C., Li, H., Li, H., Zhu, Y., & Chao, J. (2022). Effects of mixed carriers on diatomite supported nano-TiO_2. *Scientific reports*, *12*(1), 19838.

Karthikeyan, C., Arunachalam, P., Ramachandran, K., Al-Mayouf, A. M., & Karuppuchamy, S. (2020). Recent advances in semiconductor metal oxides with enhanced methods for solar photocatalytic applications. *Journal of Alloys and Compounds*, 828, 154281.

Messerer, A., Niessner, R., & Pöschl, U. (2006). Comprehensive kinetic characterization of the oxidation and gasification of model and real diesel soot by nitrogen oxides and oxygen under engine exhaust conditions: measurement, Langmuir–Hinshelwood, and Arrhenius parameters. *Carbon*, *44*(2), 307-324.

Nguyen, H. T., & Dang, P. T. (2020). Using activated diatomite as adsorbent for treatment of arsenic contaminated water. *Key engineering materials*, 850, 16-21.

Orizu, G., Ugwuoke, P., Asogwa, P., & Offiah, S. (2023). *A review on the inference of doping TiO_2 with metals/non-metals to improve its photocatalytic activities*. IOP Conference Series: Earth and Environmental Science,

Samsudin, E. M., & Abd Hamid, S. B. (2017). Effect of band gap engineering in anionic-doped TiO2 photocatalyst. *Applied Surface Science*, 391, 326-336.

Son, B. H. D., Mai, V. Q., Du, D. X., Phong, N. H., Cuong, N. D., & Khieu, D. Q. (2017). Catalytic wet peroxide oxidation of phenol solution over Fe–Mn binary oxides diatomite composite. *Journal of Porous Materials*, 24, 601-611.

Sun, W., Chu, H., Dong, B., Cao, D., & Zheng, S. (2014). The Degradation of Natural Organic Matter in Surface Water by a Nano-TiO2/Diatomite Photocatalytic Reactor. *CLEAN–Soil, Air, Water*, *42*(9), 1190-1198.

Sun, Z., Yan, Y., Zhang, G., Wu, Z., & Zheng, S. (2015). The influence of carriers on the structure and photocatalytic activity of TiO2/diatomite composite photocatalysts. *Advanced Powder Technology*, *26*(2), 595-601.

Van Pham, V., Truong, T. K., Le, H. V., Nguyen, H. T., Tong, H. D., & Cao, T. M. (2022). Enhancing green product generation of photocatalytic NO oxidation: a case of WO3 nanoplate/g-C3N4 S-scheme heterojunction. *Langmuir*, *38*(13), 4138-4146.

Van Viet, P., Van Chuyen, D., Hien, N. Q., Duy, N. N., & Thi, C. M. (2020). Visible-light-induced photo-Fenton degradation of rhodamine B over Fe2O3-diatomite materials. *Journal of Science: Advanced Materials and Devices*, *5*(3), 308-315.

Wang, X., Wang, J., Liu, S., Dou, M., & Gao, B. (2024). Sterilization mechanism and nanotoxicity of visible light-driven defective carbon nitride and UV-excited TiO2. *Journal of hazardous materials*, *461*, 132109.

Zhang, G., Wang, B., Sun, Z., Zheng, S., & Liu, S. (2016). A comparative study of different diatomite-supported TiO2 composites and their photocatalytic performance for dye degradation. *Desalination and Water Treatment*, *57*(37), 17512-17522.